

# **Investigation of Flicker Noise and Deep-Levels in GaN/AlGaN Transistors**

A. Balandin

Department of Electrical Engineering  
University of California – Riverside  
Riverside, CA 92521

K.L. Wang, S. Cai, R. Li, C.R. Viswanathan  
Electrical Engineering Department  
University of California - Los Angeles  
Los Angeles, CA 90095

E.N. Wang and M. Wojtowicz  
TRW, Inc.  
Electronics and Technology Division  
Redondo Beach, CA 90278

## **ABSTRACT**

We report flicker noise measurements combined with deep-level transient spectroscopy of the doped and undoped channel GaN/AlGaN heterostructure field-effect transistors. The low-temperature noise spectra for the doped devices show clear generation-recombination peaks. The value of the activation energy extracted from these noise peaks is consistent with the activation energies measured using deep-level spectroscopy. Our results indicate that the input-referred noise spectral density of the undoped channel devices is much smaller (up to two orders of magnitude) than that of the doped channel devices with comparable electric characteristics. The additional defects due to doping add up to the generation-recombination and flicker noise.

## I. INTRODUCTION

Advances in GaN-related compound materials and heterojunction field effect transistors (HFET) have led to demonstration of the high-power-density microwave operation of these devices. GaN HFETs exhibiting the cutoff frequency of 60 GHz and the maximum frequency exceeding 100 GHz have been recently reported by this group [1]. We have also shown that GaN HFETs grown on sapphire can operate with low flicker noise levels, which are required for the microwave applications, particularly low-phase noise amplifiers [2-3]. The flicker noise, which manifests itself at low-frequencies (usually 0.01 kHz – 100 kHz) with the  $1/f^\gamma$  spectral density dependence, is an important figure-of-merit for semiconductor devices since this type of noise is the limiting phase-noise factor for all kinds of transistors ( $\gamma$  is a parameter close to 1).

The value of flicker noise is also a good indicator of the material quality. There are two well-known models for the  $1/f^\gamma$  noise: carrier density fluctuation and mobility fluctuation models. Previous studies of the low-frequency noise in electron devices had shown that flicker noise often arises from material defects, different types of localized states, which act as carrier trapping and detrapping centers [4-6]. For example, McWhorter attributed flicker noise to the capture and emission of carriers by traps through tunneling processes [7]. The trapping and detrapping of carriers lead to fluctuations in the occupancy of the interface traps at the Fermi level which modulate the local carrier concentration. This type of noise may be superimposed over the low-frequency noise due to carrier mobility fluctuations [8]. According to the carrier trapping-detrapping model, the  $1/f$ -type noise spectral density is closely related to the Lorentzian peaks of the generation-recombination (g-r) noise. Simply put, the  $1/f^\gamma$  arises from traps with a broad distribution in energy while the g-r noise is due to discrete energy states [5].

Flicker noise in GaAs and Si transistors has been studied for several decades [9]. Although there is still no single model that could explain all the diverse results obtained under different experimental conditions, the requirements for many material systems for reducing noise are known. However, it is not the case for GaN/AlGaIn heterostructures. Very little is known about the physical origin of the low-frequency noise in GaN HFETs and the effect of the material quality on the noise level. It is also not

clear which model (the mobility fluctuation or the number fluctuation through random carrier trapping-detrapping) describes the  $1/f$  noise in the GaN system the best [10-12].

It has been previously shown that GaN/AlGaN heterostructures have large piezoelectric coefficients which lead to strong electric polarization on (0001) faces of the wurtzite structures typically used to form GaN HFETs [13-14]. The latter results in appreciable charge densities, which are large enough to design HFETs without any channel doping. Due to this reason it is important to know how the channel doping influences the low-frequency noise in GaN devices. It is particularly interesting to know if Si atoms, which are used as dopants, may form different complexes of traps in GaN/AlGaN system. It has been recently shown that the Si dopant forms two donor states in  $Al_xGa_{1-x}N$  ( $0.5 < x < 0.6$ ) [15].

In this paper we report results of the low-frequency noise measurements in the doped and undoped channel GaN/AlGaN HFETs grown on 4H-SiC or sapphire substrates. A higher aluminum content of the undoped channel devices leads to a higher piezoelectrically induced charge density, thus making up for the absence of doping and allowing for a meaningful comparison of the noise levels between the two types of devices. In order to clarify the physical origin of the low-frequency noise and understand the influence of material quality on device performance, we have conducted low-temperature noise measurements and deep-level transient spectroscopy (DLTS) studies of these devices.

The rest of the paper is organized as follows. In the next section we describe the measurement of the flicker noise in the temperature range from 77 K to 300 K. In section III, the results of the DLTS study of GaN/AlGaN transistors are presented, followed by the discussion and comparison with the activation energy extracted from the noise measurements. We give our conclusion in section IV.

## II. LOW-FREQUENCY NOISE IN GaN TRANSISTORS

It is known that *GaN* is highly piezoelectric. In a properly designed heterostructure, the lattice constant mismatch between *GaN* and  $Al_xGa_{1-x}N$  layers is accommodated by the internal strain rather than by the formation of misfit dislocations. Because of the piezoelectric effect, this strain induces an electric field and significantly changes the carrier distribution near the interface [13-14]. The latter leads to an

increase in the charge density in the two-dimensional (2D) channel. In addition, an externally doping is used in order to increase the total number of carriers.

Having these considerations in mind, we have designed two  $GaN/Al_xGa_{1-x}N$  HEMT-type structures grown on  $SiC$  substrate, in which approximately the same sheet carrier density in the 2D channel was obtained by the different means. The structure P1 was externally doped to  $N_d=2 \times 10^{18} \text{ cm}^{-3}$  and had a low piezoelectrically induced charge density due to the small  $Al$  content in the barrier layer, resulting in a small strain  $\epsilon_{xx}$  ( $\epsilon_{xx} \sim x$ , where  $x$  is the  $Al$  mole fraction). The device structure F2 was not doped externally ( $N_d=0$ ), but had a higher piezoelectrically induced charge density due to the high  $Al$  content (more than two times) used in the barrier layer. It has been experimentally shown by Asbeck *et al* [16] that the piezoelectric charge density is linearly proportional to the aluminum content in the barrier layer. As a result, the stronger piezo-effect in the structure F2 approximately made up the loss of the sheet density due to the absence of the external doping. The external doping of the barrier and channel regions, unavoidable background charges, and the piezo-effect resulted in a sheet electron concentration of about  $(1.1-1.2) \times 10^{13} \text{ cm}^{-2}$  for both device structures.

The only major differences for structures P1 and F2 were the doping density and the  $Al$  content. The layer structure of both devices was the same as used in design of high electron mobility transistors (HEMT). Details of the structure parameters and fabrication process have been reported by us earlier [2-3]. With these two types of devices, we were able to carry out a comparative flicker noise study and elucidate the effect of doping on the noise level. In addition, we have studied  $GaN$  transistors fabricated on sapphire substrate. The structure LA15 of this device was analogous to structure P1 in other respects, and was also doped [2,3].

We have examined a large number of devices with different gate widths ( $W \sim 50 \mu\text{m} - 80 \mu\text{m}$ ), gate lengths ( $L_G \sim 0.25 \mu\text{m} - 1 \mu\text{m}$ ) and different source - drain separation distances ( $L_{SD} \sim 2 \mu\text{m} - 4 \mu\text{m}$ ). For these devices, we have obtained experimental dependencies of the equivalent input referred noise power spectrum on the frequency, gate and drain voltages. The measurements were carried out for both the linear region of device operation corresponding to low drain-source voltage,  $V_{DS}$ , and at the onset of the saturation region of operation corresponding to  $V_{DS} = 5V$ . Typical DC current - voltage characteristic of  $GaN$  HFET is presented in Fig. 1. The drain-source voltage  $V_{DS}$  was used as a parameter with a step of

1V being varied from 0 V.

As we pointed out earlier, P1 and F2 devices had approximately the same carrier density in the 2D channel. At the same time, the mobility was very different for these devices. Electron Hall mobility at room temperature was determined to be  $616 \text{ cm}^2/\text{Vs}$  for the doped HFETs, and  $1339 \text{ cm}^2/\text{Vs}$  for the undoped HFETs, respectively. This significant difference is expected because the regular external channel doping introduces additional scattering centers in the channel, which deteriorates electron mobility. Despite this difference, both types of the devices had rather similar electrical characteristics (breakdown voltage  $V_{ds} > 70\text{V}$ , threshold voltage  $V_{th} = -5.5\text{V}$ , and transconductance  $g_m = 160\text{-}180 \text{ mS/mm}$ ).

The flicker noise measurements have been carried out on a regular experimental setup that consists of a low-noise amplifier, a dynamic signal analyzer and bias power supplies [4,10]. These measurements revealed a significant and important difference in the noise level in the externally doped GaN HFETs and undoped HFETs (see Fig. 2). The experimental results indicate a two-orders-of-magnitude reduction in the input-referred noise spectral density of the undoped (F2) device (with a higher piezoelectric charge density) with respect to the noise density of the externally doped channel devices (P1). The threshold voltages are  $V_T = -4.5 \text{ V}$ ,  $V_T = -5.5 \text{ V}$ ,  $V_T = -7.5 \text{ V}$  for type P1, F2, and LA15 devices, respectively. The results presented in Fig. 2 were measured in the linear regime ( $V_{DS} = 0.5 \text{ V}$ ). The difference in the low-frequency noise level is particularly significant in view of the fact that these devices have comparable characteristics, e.g., total sheet carrier concentration,  $g_m$ , and  $V_T$ . The flat regions for frequencies above 10 kHz are due to limitations of the experimental setup. At the onset of the saturation region ( $V_{DS} = 5 \text{ V}$ ), the noise spectral density for the undoped channel device is again significantly smaller than that for the externally doped channel device (see Fig. 3) with the same carrier density. The slope  $\gamma$  of the  $1/f^\gamma$  dependence in all noise power density spectra is close to 1, although the noise power varies for different devices and various gate bias values. It is important to note that the low noise value in the undoped devices with the high Al content in the barrier was observed in the subsaturation region, since GaN HFETs were designed to operate at high  $V_{DS}$ .

In order to characterize the overall “noisiness” of the devices, we have estimated the Hooge parameter several different devices made out of F2 and P1 structures. The total number of carriers in the active channel was calculated using Ohm’s law under the homogeneous channel assumption [3]. For the

devices with the gate length  $L=1\ \mu\text{m}$ , and the gate width  $W=50\ \mu\text{m}$ , we have found the following average values of the Hooge parameter  $\alpha_H$ :  $\alpha_H \sim 10^{-4}$  for the devices on structure F2, and  $\alpha_H \sim 10^{-3}$  for the devices on structure P1. As one can see a significant difference in the noise spectral density has led to an order-of-magnitude difference in Hooge parameter.

In Fig. 3, we also see a trace of the generation-recombination ( $g-r$ ) bulge in the noise spectra of the doped channel devices. The presence of the  $r-g$  peak in the saturation regime may be an indicator of the carrier trapping-detrapping mechanism of the  $1/f^\gamma$  noise in GaN/AlGaIn structure [11]. The latter served as a motivation for us to conduct a low-temperature study of the noise in GaN HFETs in order to determine the trap activation energy and compare the value with that extracted from DLTS study.

The low temperature noise characteristics of the doped and undoped channel devices were examined in the temperature range from 77K to 300K. Fig 4. shows these characteristics in the linear region of operation for the device F2. There are no clear signs of a  $r-g$  peak for either of the device types. In the subsaturation region, a pronounced peak was observed at about 3-4 kHz for the doped channel devices (see Fig. 5). At the same time, no peak in spectra of the undoped channel device was observed. On the contrary, the 77K spectrum of the undoped channel GaN HFET flattens at the corner frequency of about 1 kHz anticipated due to the Johnson noise. The level of the Johnson noise of  $6 \times 10^{-16}\ \text{V}^2/\text{Hz}$  is in agreement with the value estimated from the Nyquist formula. Fitting the Lorentzian shape, we have extracted the activation energy of about 0.35 eV. The fitting procedure was based on the method described in Ref. [17]. One should also note that  $\gamma > 1.2$  for the undoped device. This unusual behavior can be attributed to several possible reasons. One of them is temperature fluctuation during the measurements for each given gate bias (the temperature was drifting to lower values as the frequency was increasing). Another possible explanation may be related to a particular trap density distribution, which in our case is strongly non-uniform. It was shown in Ref. [18] that  $\gamma$  parameter may vary in wide range depending on the distribution of the tunneling time constants for the carrier trapping – detrapping processes.

### III. DEEP LEVEL TRANSIENT SPECTROSCOPY OF GaN/AlGaIn TRANSISTORS

Although noise spectroscopy has been used for many years to study deep levels in semiconductors, it is the deep-level transient spectroscopy (DLTS) that gives direct characteristics of deep level defects. DLTS measures the capacitance or current change of a reversed biased junction when deep levels emit their carriers after they were charged by a forward bias pulse. From the temperature dependence of the emission rate, the activation energy of a deep level can be deduced. Since flicker noise in the GaN/AlGaN system is most likely related to the carrier capture and emission by some traps, we used DLTS to probe the defects.

The observation of a g-r peak in the low-temperature noise spectra of doped channel devices was an indication for the presence of some carrier traps. For this reason, we mostly concentrated our DLTS study on the doped channel GaN HFETs grown on both SiC and sapphire. A particular type of measurements, that we have carried out was Fourier Transform current deep level transient spectroscopy (I-DLTS). The devices were biased in the same configuration as they would be in a circuit. Then the gate was used to pulse the drain-source current and the transient of the current pulse was used in a manner similar to the capacitance transient in DLTS. The spectra were recorded using a pulse width  $t_p$  from 100  $\mu$ s to 1 ms. In Fig 6. We present a typical DLTS Arrhenius plot of  $T^2\mathcal{E}$  vs  $1/T$ , where  $\mathcal{E}$  is the emission rate at a temperature  $T$ . The data are shown for the GaN doped channel HFET grown on SiC (P1). From this Arrhenius plot we have extracted an activation energy  $E_a=0.201$  eV below the conduction band.

The results of the DLTS study for other samples are summarized in Table I. The bias conditions for the measurements were the following: the source – drain voltage  $V_{DS}=1$ V for all devices; the reverse and forward biases  $V_R=-7.5$  V and  $V_P=5.0$  V for LA15 HFETs; and  $V_R=-4.0$  V and  $V_P=3.0$  V for P1 HFETs. The values of the activation energy shown here are rather typical for the examined devices. From these values, one can conclude that the carriers are indeed trapped and detrapped by the deep level and not by the Si shallow states. It is also interesting to note that HFETs on sapphire substrate has an obviously higher activation energy ( $E_a \sim 0.85$  eV) than that of the device on SiC ( $E_a \sim 0.20$  eV - 0.36 eV). The origin of this difference in the deep level activation energy is not clear. Recall that both types of devices were doped with Si and had a similar structure (see Refs. [2,3,10] for details of the layer structure); devices grown on sapphire and SiC had approximately the same flicker noise level provided that the device parameters (source-drain separation, gate length, width, etc.) were close. One possible

explanation may be that these traps are not related to Si dopants but are due to some other defects introduced during growth, which are different for structures grown on SiC and sapphire substrates.

The values of the activation energy obtained by us for the P1 device are close to the ones reported by Auret *et al.* [19]. They have studied proton bombardment-induced electron traps in epitaxially grown *n*-GaN. In their DLTS study of the control (not bombarded) sample, energies of 0.21 eV, 0.27eV, and 0.45eV have been obtained. At least two of these values are in agreement with our observations (see Table I).

Since the activation energy ( $E_a \sim 0.35$  eV) extracted from the low-temperature flicker noise spectral density is close to the DLTS value, it is reasonable to assume that carrier trapping-detrapping is a dominant noise mechanism in the doped GaN/AlGaN structure. At the same time, it is still not possible to exactly identify the origin of deep levels and their contribution to the flicker noise. The significant difference in the measured activation energies for the doped devices grown on SiC and sapphire substrates seems to suggest that these defects may have different origins.

#### IV. CONCLUSIONS

We have carried out low-frequency noise measurements combined with deep level transient spectroscopy (DLTS) of the doped and undoped channel GaN/AlGaN heterostructure field-effect transistors. The increased aluminum content in the barrier region of the undoped devices compensated for the loss of the sheet carrier density due to the absence of the external doping, and has led to the carrier density in the channel comparable to that induced by external doping. The low-temperature noise spectra for doped devices show a clear generation-recombination peak in the subsaturation region. The value of the activation energy extracted from these noise peaks is consistent with the activation energy found in our DLTS study. The latter may be responsible for the carrier trapping-detrapping, which induces the low-frequency noise in the GaN/AlGaN devices. Our results indicate that the input-referred noise spectral density of the undoped channel devices is much smaller (up to two orders of magnitude) than that of the doped channel devices with comparable electric characteristics. It was also determined that the characteristic energy of the deep levels in GaN devices grown on SiC substrates is different from that one of the devices grown on sapphire.

## **ACKNOWLEDGEMENT**

The work in UCLA was supported in part by the DoD MURI-ARO program on Low Noise Electronics. The authors thank Dr. S. Morozov (Institute of Microelectronics, Russian Academy of Sciences) and Mr. G. Wijeratne (UCLA) for their help in noise measurements.

## REFERENCES

- [1]. S.J. Cai, R. Li, Y.L. Chen, L. Wong, W.G. Wu, S.G. Thomas, and K.L. Wang, *Electron. Lett.*, **34**, 2354 (1998).
- [2]. A. Balandin, S. Cai, R. Li, K.L. Wang, V. Ramgopal Rao, and C.R. Viswanathan, *IEEE Electron Device Lett.*, **19**, 475 (1998).
- [3]. A. Balandin, S.V. Morozov, S. Cai, R. Li, K.L. Wang, G. Wijeratne, and C.R. Viswanathan, *IEEE Trans. Microwave Theory and Tech.*, **47**, 1413 (1999).
- [4]. J. Chang, A.A. Abidi, C.R. Viswanathan, *IEEE Trans. Elec. Devices*, **41**, 1965 (1994).
- [5]. W.Y. Ho, C. Surya, K.Y. Tong, W. Kim, A. E. Bochkarev, H. Markoc, *IEEE Trans. Elec. Devices*, **46**, 1099 (1999).
- [6]. N.V. Dyakonova and M.E. Levinshtein, *Sov. Phys. Semicond.*, **23**, 175 (1989).
- [7]. A.L. McWhorter, in *Semiconductor Surface Physics*, (Philadelphia, University of Pennsylvania Press, 1957), Ed. R.H. Kingston, p. 207.
- [8]. A. Balandin, K.L. Wang, A. Svizhenko, S. Bandyopadhyay, *IEEE Trans. Elec. Devices*, **46**, 1240 (1999).
- [9]. A. van der Ziel, *Proc. IEEE*, **76**, 233 (1988).
- [10]. A. Balandin, S. Morozov, G. Wijeratne, S.J. Cai, R. Li, J. Li, K.L. Wang, C.R. Viswanathan, and Yu. Dubrovskii, *Appl. Phys. Lett.*, **75**, 2064 (1999).
- [11]. M.E. Levinshtein, F. Pascal, S. Contreras, W. Knap, S.L. Rumyantsev, R. Gaska, J.W. Yang, M.S. Shur, *Appl. Phys. Lett.*, **72**, 3053 (1998).
- [12]. D.V. Kuksenkov, H. Temkin, R. Gaska, and J.W. Yang, *IEEE Electron. Device Lett.*, **19**, 222 (1998).
- [13]. A. Bykhovski, B. Gelmont, M. Shur, *J. Appl. Phys.*, **74**, 6734 (1993).
- [14]. A. Bykhovski, B. Gelmont, M. Shur, *J. Appl. Phys.*, **81**, 6332 (1997).
- [15]. C. Skierbiszewski, T. Suski, M. Leszczynski, M. Shin, M. Skowronski, M.D. Bremser, R.F. Davis, *Appl. Phys. Lett.*, **74**, 3833 (1999).
- [16]. P.M. Asbeck, E.T. Yu, S.S. Lau, G.J. Sullivan, J. Van Hove, J. Redwing, *Electron. Lett.*, **33**, 1230 (1997).

A. Balandin, *et. al.*, *J. Electron. Materials*, **29**, 297 (2000).

[17]. J.R. Kirtley, T.N. Theis, P.M. Mooney, and S.L. Wright, *J. Appl. Phys.*, **63**, 1541 (1988); Y. Haddab, B. Deveaud, H.-J. Buhlmann, and M. Ilegems, *J. Appl. Phys.*, **78**, 2509 (1995).

[18]. C. Surya, T.Y. Hsiang, *Phys. Rev. B*, **33**, 4898 (1986).

[19]. F.D. Auret, S.A. Goodman, F.K. Koschnick, J.-M. Spaeth, B. Beaumont, P. Gibart, *Appl. Phys. Lett.*, **74**, 407 (1999).

## FIGURE CAPTIONS

Figure 1. Typical DC current-voltage characteristics of the GaN HFET (P1).

Figure 2. Input referred noise spectral density for the doped channel device (empty squares and circles) and undoped channel device (filled squares and circles) with a higher aluminum content in the barrier. Data are shown for the linear regime of operation. A significant difference in the noise density was observed for all values of the gate biases. The device dimensions are  $L \times W = 1 \mu\text{m} \times 50 \mu\text{m}$ .

Figure 3. Input referred noise spectral density for the doped channel device (circles) and undoped channel device (rectangles) with higher aluminum content in the barrier. Data are shown for the subsaturation regime of operation. A significant difference in the noise density was observed for all values of the gate bias (shown for the gate bias  $V_{GS} = -4 \text{ V}$ ).

Figure 4. Low-temperature noise characteristics of GaN HFET (F2) in the linear region of operation. No generation – recombination peaks were observed.

Figure 5. Low-temperature noise characteristics of GaN HFET in the subsaturation region of operation. One can clearly see the generation – recombination peak. The activation energy extracted from the low-temperature noise data was compared with the DLTS deep level signatures.

Figure 6. Results of DLTS measurements shown for GaN HFET grown on SiC substrate. The time constant for this measurement was  $t_p = 100 \mu\text{s}$ .

	LA15 (A)	LA15 (B)	P1 (A)	P1 (B)	P1 (C)
E, eV	0.854	0.846	0.201	0.288	0.365
$t_p$ , $\mu$ s	100.0	100.0	100.0	100.0	100.0

Table I. Results of DLTS study for GaN/AlGaN HFETs on SiC (P1) and sapphire (LA15) substrates

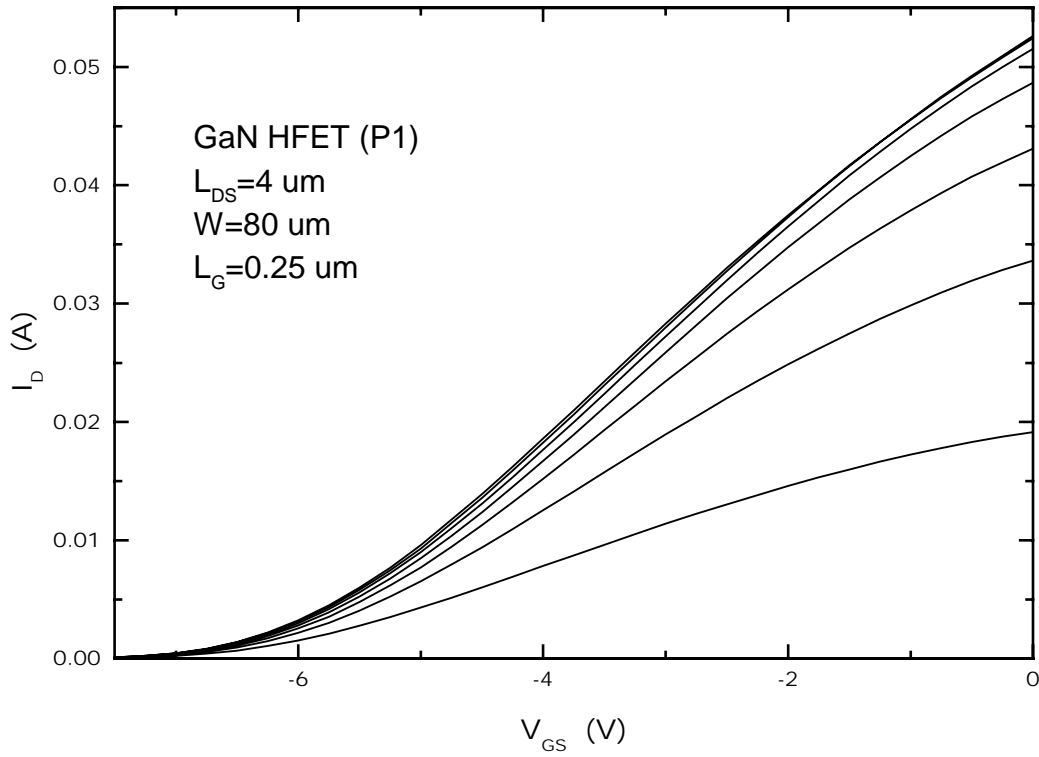


Figure 1. Balandin et al., JEM.

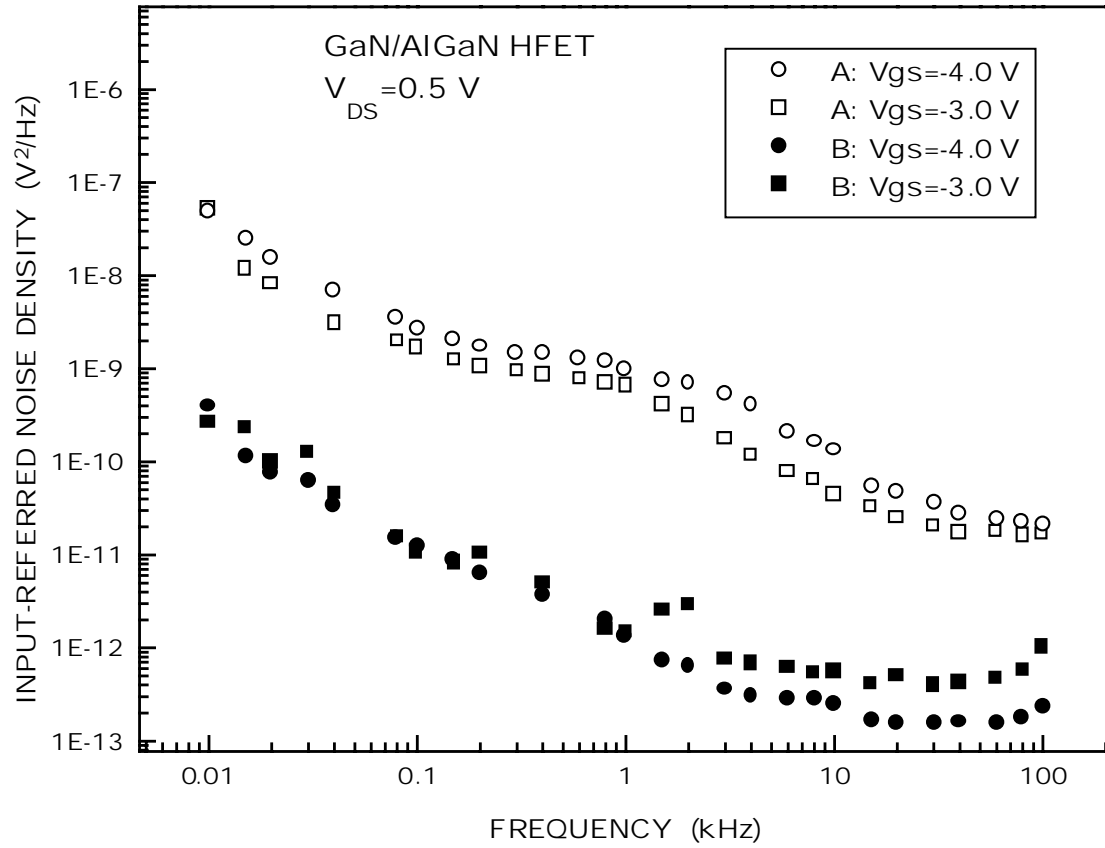


Figure 2. Balandin et al., JEM.

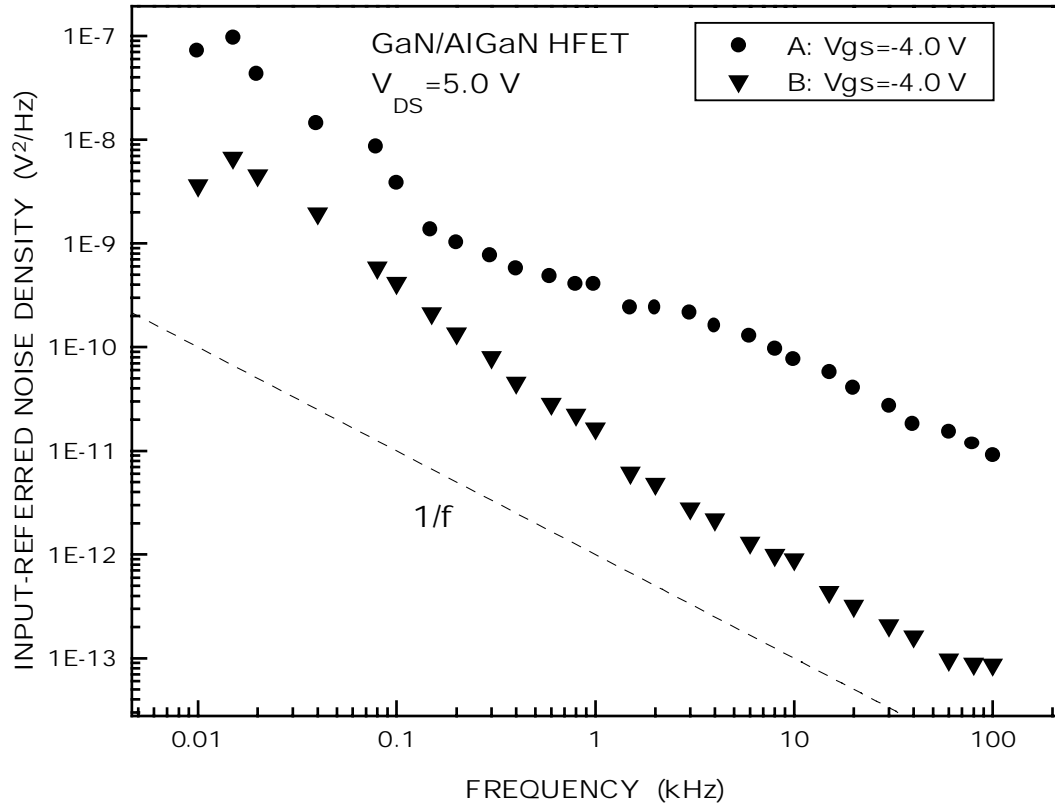


Figure 3. Balandin et al., JEM.

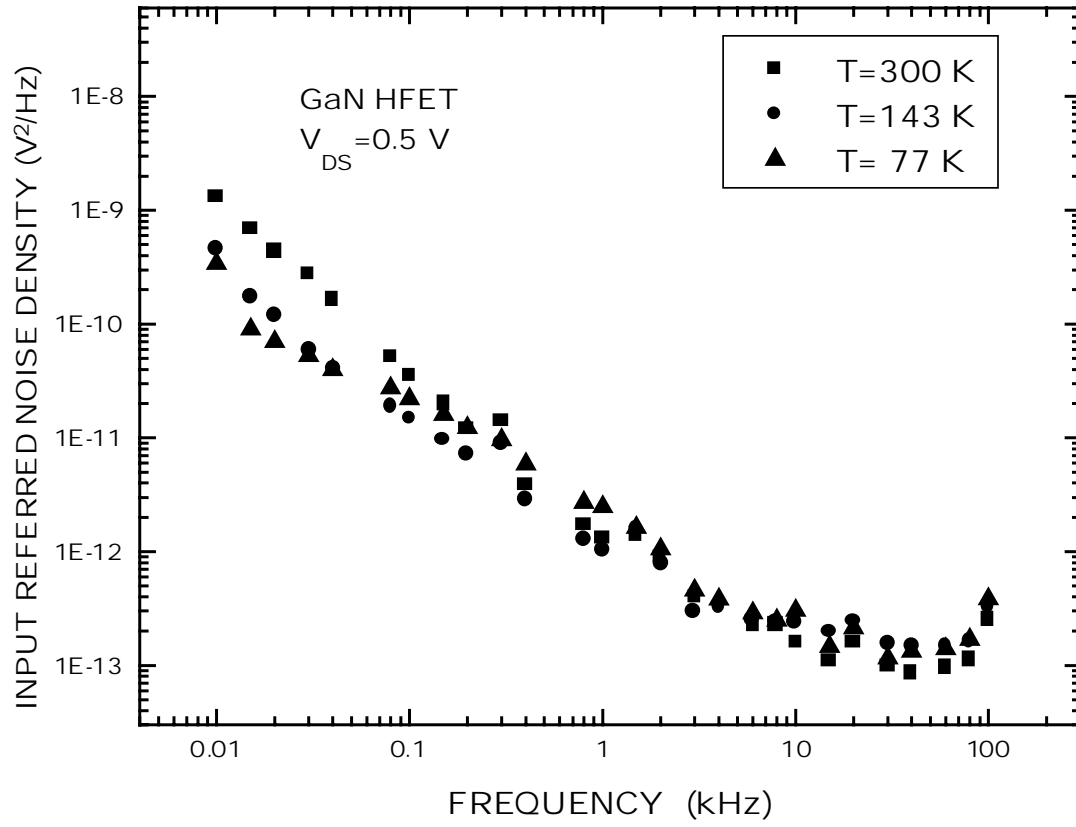


Figure 4. Balandin et al., JEM.

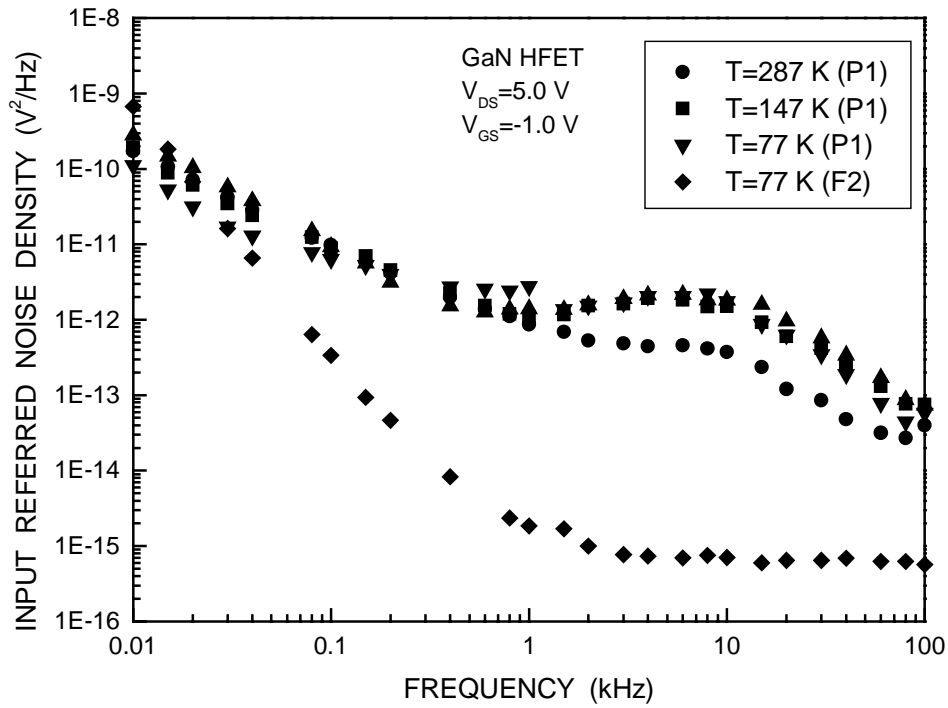


Figure 5. Balandin et al., JEM.

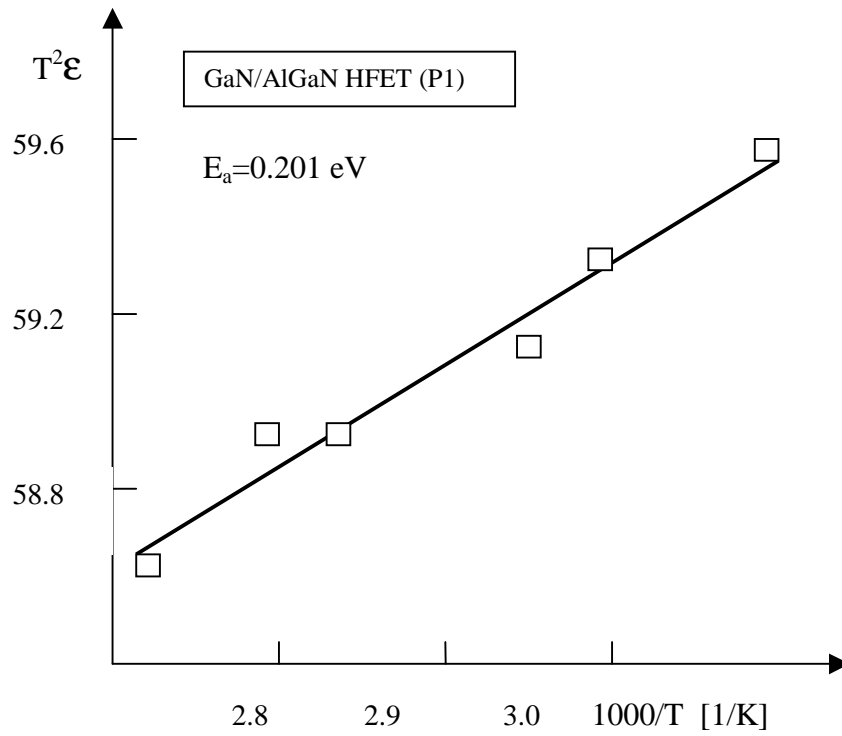


Figure 6. Balandin et al., JEM.